Reprinted from JOURNAL OF STATISTICAL PHYSICS Vol. 76, Nos. 5/6, September 1994
Printed in Belgium

The Dynamics of Defect Ensembles in One-Dimensional Cellular Automata

Kari Eloranta[1]

Received November 8, 1993; final May 17, 1994

We investigate the dynamics of ensembles of diffusive defects in one-dimensional deterministic cellular automata. The work builds on earlier results on individual random walks in cellular automata. Here we give a natural condition guaranteeing diffusive behavior also in the presence of other defects. Simple branching and birth mechanisms are introduced and prototype classes of cellular automata exhibiting weakly interacting walks capable of annihilation and coalescence are studied. Their equilibrium behavior is also characterized. The design principles of cellular automata with desired diffusive interaction properties become transparent from this analysis.

KEY WORDS: Cellular automaton; permutivity; topological defect; random walk.

INTRODUCTION

Topological defects, Bloch walls, or contours can be identified in a number of standard lattice models in statistical mechanics. They are boundaries between adjacent domains/phases and since their motions determine the macroscopic properties of the medium to a large extent their analysis has attained a central position in the discipline.[8,3,15]

Cellular automata (CA), being a discretized form of lattice dynamics, are believed to share common properties with numerous statistical mechanics models.[9,2] While introducing some novelty and simplicity, their purely discrete and deterministic nature also introduces combinatorial difficulties in the analysis in comparison to the standard probabilistic models.

[1] Institute of Mathematics, Helsinki University of Technology, 02150 Espoo, Finland.

0022-4715/94/0900-1377$07.00/0

In this study we investigate large classes of deterministic one-dimensional CA which exhibit surprisingly "physics-like" phenomena in the aforementioned sense. In particular they support phase boundaries performing random walks. The basic phenomenology as well as complete and rigorous characterization of individual motions were the subject of our earlier work.[5,6] Here the focus is on ensembles of interacting random walks which either were originally present or are born from vacuum or branch from existing ones at a given rate. In contact interaction they recombine either by annihilating or coalescing, depending on their types. We single out prototype classes of partially permutive CA where the interaction is weak enough so that the global action is still diffusive and analyzable. It turns out that the behavior of the CA is quite predictable from the design. This by itself is novel in the context of CA, where combinatorial details often tends to erase any continuity from the parameters. Hence it is perhaps justified to view our setup and parametrizations as natural for the problem.

Indeed our claim is that the structures unveiled here are the very reason why the commonly used notion "statistical mechanics of CA" makes sense.

One could also view the results as an ideal way of generating pseudorandom lattice dynamics. This is because by their very nature CA are computationally extremely efficient and just seed randomness is needed to be injected using standard algorithms.

The work is structured as follows. We first note the basic definitions and dynamics types. In Section 2 we define the prototype classes of CA. This involves the key reformulation of a CA rule which essentially decodes it to a stationary process and a symbolic flow on it. In this setup the motion as well as the branching properties of an individual boundary point have natural characterizations. The critical permutivity property of the underlying dynamics is then connected to some recent investigations on $\mathbf{Z}^2$-actions.

In the beginning of Section 3 we present some empirical results concerning the classes under consideration in the various cases involving different birth and branching intensities. These results are then compared with predictions of probabilistic models derived using Feynman-type path decomposition and independence assumptions. The conservation laws inevitable in the context of deterministic CA are then analyzed. Finally we formulate a conjecture related to the equilibrium states of the classes. The conjecture is connected to earlier work on simpler dynamics with stronger assumptions. Along the way, we also discuss the dynamics resulting from relaxing the permutivity structure, quenching the seed randomness, etc.

1. PRELIMINARIES

The presentation here is a rather terse but still self-contained. Elaboration on the basic concepts can be found in earlier parts of this paper sequence.[5,6]

Let S be a finite set of *symbols* and $X = \underline{S} = S^{\mathbf{Z}}$ and $X^{(1/2)} = \underline{S}^{(1/2)} = S^{Z+1/2}$ the sets of *configurations*. If the *left shift* σ is defined for any $x \in X^{(\cdot)}$ by $(\sigma x)_j = x_{j+1}$, then we can define our object of study.

Definition 1.1. A map $f: S \times S \to S$ on neighboring symbols is a *cellular automaton rule*. It commutes with the left shift and thereby induces a global *cellular automaton map* $F: X \to X^{(1/2)}$ and $F: X^{(1/2)} \to X$.

Every one-dimensional CA is of this form.[5]

Definition 1.2. A set $S^{(a)} \subset S$ is called *right-invariant* if $f(s, S^{(a)}) = S^{(a)}$ for all $s \in S^{(a)}$, i.e., $f(s, \cdot)$ is a permutation on $S^{(a)}$. *Left invariance* is defined in a symmetric fashion. If the permutivity holds on both sides, the map is *permutive on* $S^{(a)}$.

The index in $S^{(a)}$ refers to our convention that S splits into *subalphabets*. We denote their set by $A = \{0, 1, \ldots\}$. To obtain necessary closure properties, we now make a basic assumption.

Assumption 1.3. In this study we assume that for $a \neq a'$, $S^{(a)} \cap S^{(a')} = \varnothing$ and $S = \bigcup_A S^{(a)}$. We also restrict ourselves to the case $|S^{(a)}| = q \geqslant 2$, i.e., the subalphabets are nontrivial and of equal size.

The assumption on disjointness implies that for any $s \in S$ there is a unique a s.t. $s \in S^{(a)}$, thereby ruling out the existence of *ambiguous symbols*. However, any rule with ambiguous symbols can be naturally extended to a rule without ambiguous symbols.[6] We do not expect the size difference of the subalphabets to introduce genuinely new interaction phenomena.

Clearly all configurations *generated* from a single invariant subalphabet, i.e., $X^{(a)} = S^{(a)\mathbf{Z}}$ (or the ones on half-integers) are invariant subsets of X (or $X^{(1/2)}$) under F^2 and it seems appropriate to call them *pure phases*.

Definition 1.4. Given $l, r \in A$, $l \neq r$, a configuration $x \in X$ s.t. $x_{j'} \in S^{(l)}$ for $j' \leqslant j$ and $x_{j'} \in S^{(r)}$ for $j' > j$ is said to have a *boundary point* at $j + 1/2$. The set of all such configurations is denoted by $\underline{S^{(l)}S^{(r)}}(j)$.

In the case of a single boundary point (as in this definition), its motion is under rather general conditions a random walk. The objective of this paper is to investigate the joint motion of an arbitrary number of boundary

points between adjacent pure phases when in the absence of others they would be performing random walks.

The contact interaction and transformation types of the boundary points are as follows.

Definition 1.5. Suppose that we have a boundary point $[s^{(l)}s^{(r)}]$, $s^{(a)} \in S^{(a)}$, $r \neq l$ at j. If $f(s^{(l)}, s^{(r)}) \in S^{(c)}$ and $c \in \{l, r\}$, the interaction is *inert* and the boundary point moves in the next iteration of F either to the left or to the right by 1/2. If $c \notin \{l, r\}$, the boundary point *branches* and we will have boundary points at $j \pm 1/2$ at the next iterate. Conversely, suppose that we have a block $[s^{(l)}s^{(c)}s^{(r)}]$ centered at the site j and $c \notin \{l, r\}$, i.e., we have two adjacent boundary points at $j \pm 1/2$. Then if under F this block maps into $[\tilde{s}^{(l)}\tilde{s}^{(r)}]$ and $l = r$ the boundary points *annihilate*. If $l \neq r$, they *coalesce* into a boundary point at j.

For branching and coalescing we obviously need $|A| \geqslant 3$.

As indicated in earlier empirical studies,[9,2] it is quite natural to interpret a boundary point either as a "particle" moving on a background defined by a pure phase or as a "crack" between a phase and its shift. In our setup the *type* of a particle is defined by the subalphabets it borders. This in turn defines its relation to the other particles, i.e., the interaction algebra determining which collisions result in annihilation and which in coalescence into a particle of a third type as well as which particle types a given particle can branch into (see Fig. 2).

2. THE PROTOTYPES

We now define the detailed structure of the CA with the desired interaction properties. The two basic ideas in this description are natural consequences of the CA being defined via a two-block rule. First by Definition 1.1 the CA rule as we define it is equivalent to a *Cayley table* or multiplication table on the symbol set S. Second this matrix naturally gives rise to a graph which supports a simple random process, which in turn determines all the properties of the boundary motion.[6] In order to keep things simple, we first consider some examples, after which it should be clear how a more general class of examples is constructed.

Example 2.1. Consider the Cayley tables in Table I indexed as matrices by $S_6 = \{1, 2, 11, 12, 21, 22\}$ on the left and $S_9 = \{1, 2, 3, 11, 12, 13, 21, 22, 23\}$ on the right.

Remark. A 4×4 Cayley table with similar structure would be the simplest CA to exhibit nontrivial interaction dynamics: annihilations (but

Table I

1	2	1	12	21	2
2	1	12	1	2	21
1	12	11	12	11	22
12	1	12	11	22	11
21	2	11	22	21	22
2	21	22	11	22	21

1	2	3	21	2	13	11	2	23
2	3	1	12	23	1	22	13	1
3	1	2	3	11	22	3	21	12
21	12	3	11	12	13	1	12	23
2	23	11	12	13	11	22	3	11
13	1	22	13	11	12	13	21	2
11	22	3	1	22	13	21	22	23
2	13	21	12	3	21	22	23	21
23	1	12	23	11	2	23	21	22

no coalescings) between boundaries of two phases. The sizes of our examples are chosen to enable all possible interaction and transformation types to appear.

Both tables correspond to a CA with three invariant subalphabets as indicated by the subsquares on the main diagonal. These are nonoverlapping matrices by Assumption 1.3 and of size 2×2 on the left and 3×3 on the right. By examining the six off-diagonal subsquares in the Cayley table one concludes that the left automaton has inert interaction between the boundary points. Furthermore, their structure is such that given the appropriate independent initial distribution, each of the boundary motions generated is a standard unbiased random walk with i.i.d. increments (see Theorem 2.4). As indicated in Definition 1.5, the possible interactions are now annihilations and coalescings. An 80-step evolution on an 80-cell torus starting from an independent and uniformly distributed sample with symbols from S_6 are shown in the upper left corner in Fig. 1 (time runs downward). Here 1 is white, 11 is gray, and 22 is black and the remaining three symbols have a slightly different shade.

The rule corresponding to the right matrix is potent: in the six off-diagonal 3×3 matrices the diagonal entries do not belong to the same subalphabets as the interacting symbols. Hence branching results at the corresponding boundary pair. However conditioned that the boundary pair avoids the subdiagonals, the rule again generates unbiased random walks with i.i.d. increments. The branching intensity (the frequency of branchings on a typical path) is 1/3. An 80-step sample is shown on the left in the middle row of Fig. 1 (initial configuration distributed as above with symbols from S_9). The rest of the illustration is explained in Section 3.1.

In the case of multiple boundary motions a useful functional representation of the interaction of the boundary point types is the graph on the left in Fig. 2. Here we denote $S^{(a)}$ simply by a, hence $\underline{aa'}$, $a \neq a'$ stands for a boundary point between phases of type $S^{(a)}$ and $S^{(a')}$ ordered that way.

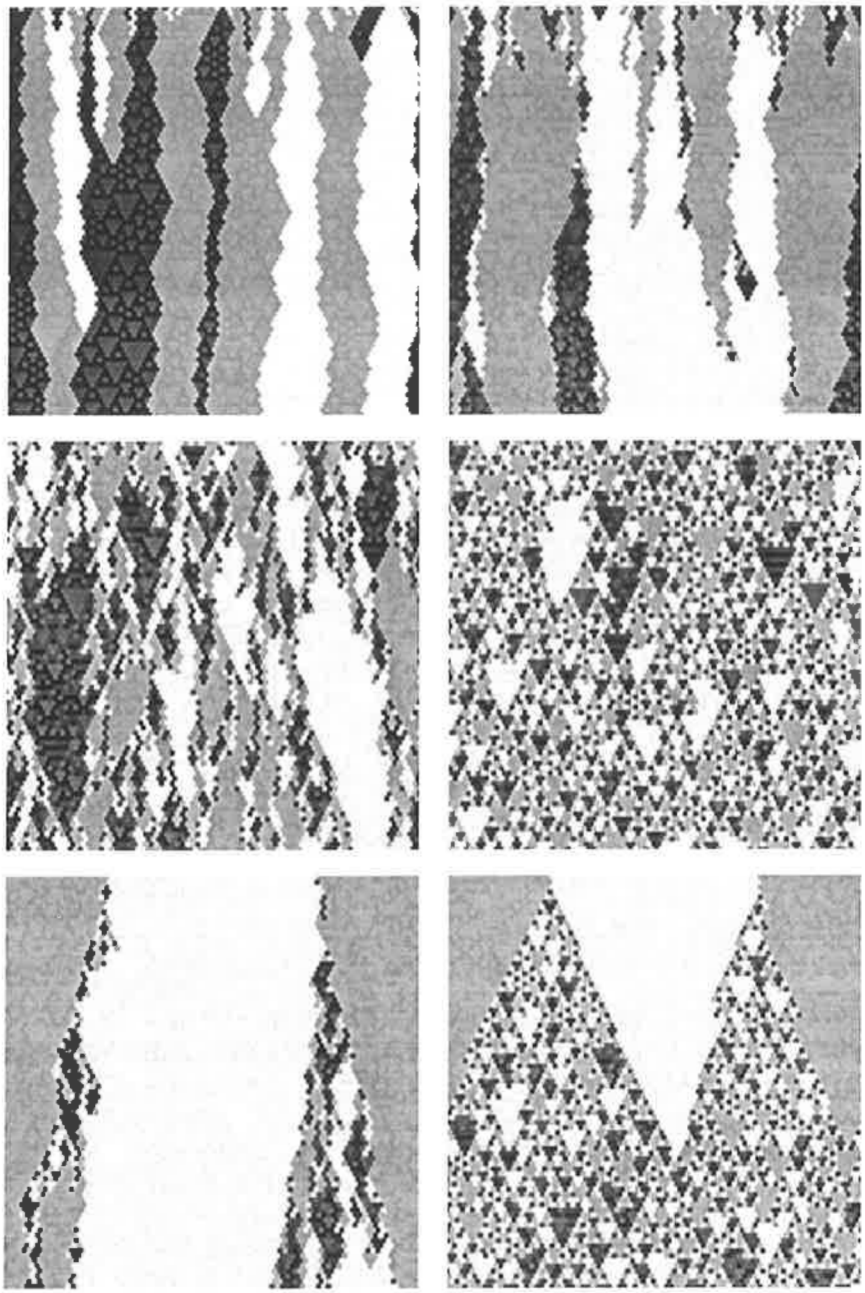

Fig. 1. Cellular automata evolutions. Toral boundary condition, time runs downward. Rules: Top left, $\mathscr{AC}$ (see Example 2.1); top right, $\mathscr{ABC}$, $b = 1/9$; center left and right, $\mathscr{ABC}$, $b = 1/3$ and 7/9; bottom row like the middle with special initial condition (for details of last five see Section 3.1).

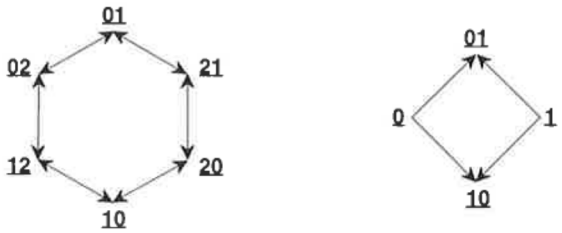

Fig. 2. Transformation of the boundary point types. Left: branchings and coalescings; right: births and annihilations.

The graph describes boundary point generation properties. For example, the arrow pair departing from 01 to 02 and 21 represent the branching potential of the corresponding boundary motion. So the inert CA in our first example corresponds to a completely disconnected graph on six vertices, while the other one is functionally like the graph on the left in Fig. 2. In the case of multiple subalphabets with different branching properties this representation can be used in ordering them as well as finding functionally equivalent CA. Transversing the same arrow pairs in the opposite directions gives the recombination of types in coalescings. The graph on the right in Fig. 2 is a similar representation of another phenomenon, spontaneous birth, in the case of two noninvariant subalphabets (for definition see end of this section).

We now generalize these examples and formulate the classes of automata on which we concentrate for most of the paper.

Let each $s \in S^{(a)}$ be represented by $s = (a, d)$, where $d \in D$. We call D the set of *digits*. By Assumption 1.3 we can choose $D = \{1, 2, \ldots, q\}$. Let

$$\underline{A} = \{A^{(a,a')}\}_{(a,a') \in A \times A} \quad \text{and} \quad \underline{\underline{Q}} = \{Q^{(a,a')}\}_{(a,a') \in A \times A}$$

where $A^{(a,a')}$ are $q \times q$ matrices whose entries are in A. The array $\underline{A}: A \times A \times D \times D \to A$ is called the *assignment matrix*. $Q^{(a,a')}$ is a $q \times q$ matrix with entries in D, i.e. it is a Cayley table on the set of digits. For simplicity we will subsequently consider the case $Q^{(a,a')} \equiv Q$ unless indicated otherwise.

With these definitions the rule of the CA is given by $f = f(\underline{A}, \underline{\underline{Q}})$ such that for $s = (a, d)$ and $s' = (a', d')$

$$f(s, s') = (A^{(a,a')}(d, d'), Q^{(a,a')}(d, d'))$$

So if, for example, $A^{(a,a')}(d, d') \in \{a, a'\}$ for all a, a', d, d', then the rule is inert, whereas if we have $\notin$ for some a, a', d, d' the boundary between these symbols will branch. Note that the invariance of the subalphabets implies that $A^{(a,a)}(d, d') \in A$ for all a, d, d'.

The idea behind this formulation is the following. If we have a way of guaranteeing that *the digit pair* (d, d') *in the boundary pair* $(s, s') =$

$((a, d), (a', d'))$ *is uniformly distributed in* $D \times D$, then with the assignment matrix we can, in a simple fashion, control the motion of the boundary point as well as its branching.

To ensure the desired distribution property for (d, d'), the Cayley tables $Q^{(a,a')}$ must have a special structure.

Definition 2.1. A Cayley table Q on the set D is a *quasigroup* if in the equation $Q(d_1, d_2) = d_3$, $d_i \in D$, any two digits uniquely determine the third.

The quasigroup structure obviously implies the permutivity of f on the subalphabets. A quasigroup does not need to be a group, nor does it have to have an identity. In the subsequent analysis we assume that Q is symmetric, which does not restrict us to groups, but makes certain arguments more transparent.

To generate the random walks, we introduce a random component in the form of the initial distribution. The notations μ_S and μ_D denote the uniform Bernoulli (product) measure on $S^{\mathbf{Z}}$ and $D^{\mathbf{Z}}$, respectively. Let the measures on the $\mathbf{Z} + 1/2$-lattice be denoted analogously with superindex $(1/2)$. The mechanism responsible for propagating the randomness to future iterates is a certain $\mathbf{Z}^2$-action which we now describe.

Let P be the global CA map that the permutive rule Q induces on the configurations generated from D. It preserves the appropriate measures, i.e., $\mu_D = \mu_D^{(1/2)} P^{-1}$, i.e., the $D^{\mathbf{Z}}$ sequences will remain independent and uniformly distributed under P. The set of all possible infinite space-time-evolutions of P is a subshift of finite type which we denote by $D^{(2)}$. Let its horizontal and vertical coordinate shifts be σ_h and σ_v. The former is defined by $(\sigma_h y)_{(j,i)} = y_{(j+1,i)}$, $y \in D^{(2)}$, and the latter by $(\sigma_v y)_{(j,i)} = y_{(j+1/2, i+1)}$, $y \in D^{(2)}$. Together they define a $\mathbf{Z}^2$-action $\sigma^{(i,j)}$ by $(j, i) \mapsto \sigma_h^j \sigma_v^i$. By taking into account the measure preservation we obtain a dynamical system $(D^{(2)}, \sigma^{(\cdot,\cdot)}, \mu^{(2)})$ (the inverse limit[14]).

Theorem 2.2. The $\mathbf{Z}^2$-action is mixing, i.e.,

$$\lim_{|i| + |j| \to \infty} \mu^{(2)}(\sigma^{(i,j)}(A) \cap B) = \mu^{(2)}(A)\, \mu^{(2)}(B)$$

for any measurable A, $B \in D^{(2)}$.

The theorem has appeared in various forms, e.g., in refs. 12, 11, and 16. The interesting question from our point of view is whether the mixing property is good enough—will the underlying digit evolution which determines the jumps of the boundary point produce sufficiently weakly interacting motions so that they will retain their random walk character? We elaborate this question throughout the rest of the paper.

We are now ready to define the prototype assignment matrices and thereby the CA. Let ϕ be the cyclic permutation $0 \mapsto 1 \mapsto 2 \mapsto 0$.

Definition 2.3. Suppose $|A| = 2$ or 3 and $|D| \geqslant 2$ is even. Let $A^{(0,1)}$ be symmetric and such that half of each row is 0's and half 1's and let $A^{(1,0)} = A^{(0,1)}$. If $|A| = 3$ define the rest of $\underline{A}$ by

$$A^{(\phi^i(0),\phi^i(1))}(d, d') = \phi^i(A^{(0,1)}(d, d')), \qquad i = 1, 2, \quad \forall d, d' \in D$$

By letting $Q^{(a,a')} \equiv Q$, we define a class of symmetric CA rules which we call $\mathscr{AC}$.

Remarks. The name refers to the fact that for $|A| = 2$ these inert CA are capable of generating annihilating random walks and in the case $|A| = 3$ also coalescing ones. A checkerboard covering with 0's and 1's is a natural choice for $A^{(0,1)}$. Note that by the symmetry of $A^{(\cdot,\cdot)}$, $\underline{A}$ is symmetric, i.e., $A^{(a,a')}(d, d') = A^{(a',a)}(d', d)$, hence by the symmetry of $\underline{Q}$, f also is symmetric. The matrix on the left in Table I is an example of $\mathscr{AC}$ ($Q = \mathbf{Z}_2$ and $A^{(0,1)}$ a checkerboard).

The class generates good individual boundary motions. Let π_1 and π_2 be the projections of a measure on X on $A^{\mathbf{Z}}$ and $D^{\mathbf{Z}}$, respectively.

Theorem 2.4. Let the measure μ be a measure supported on $\underline{S^{(0)}S^{(1)}}(j_0)$, j_0 an integer or half-integer and $\pi_2\mu = \mu_D$. Given a rule in $\mathscr{AC}$, the boundary point performs an unbiased random walk with i.i.d. increments and unit variance 1/4.

Proof. Without loss of generality we can choose $|A| = 2$. Suppose that the defect at time i is at j_i. Consider the triangle T_i with vertices at $(j_i, i+1)$ and $(j_i \pm (i+1)/2, 0)$. Define the backward cone of the boundary pair centered at j_i at time i to be the set $T_i \backslash \{(j_i, i+1)\}$. The past of the walk at time i is clearly contained in this backward cone and the cone determines the next jump, i.e., value of the cell at $(j_i, i+1)$. Suppose that the walk jumps to the right, i.e., the cell at $(j_i, i+1)$ is in $S^{(0)}$. We claim that given the backward cone at time i, the value of the neighbor at $(j_i+1, i+1)$ is determined permutively by the entry at $(j_i + (i+3)/2, 0)$. This follows by noting that as $(j_i + (i+1)/2, 0)$ is now fixed, $(j_i + (i+3)/2, 0)$ permutes $(j_i + (i+2)/2, 1)$ and then iterating this argument i times. So the next jump is independent of all the previous ones. Moreover, as the digit at $(j_i + (i+3)/2, 0)$ is uniformly distributed, so is the digit at $(j_i+1, i+1)$. By the column structure of $A^{(0,1)}$ in $\mathscr{AC}$ the jumps to both directions take place with probability 1/2. Therefore the unit variance is simply $1/2(-1/2)^2 + 1/2(1/2)^2 = 1/4$. ■

Remark. More complex f arrays can be dealt with using a graph formulation.[6] In order not to obscure the main points, we refrain from defining the most general analyzable classes here.

Definition 2.5. Suppose $|A| = 3$ and $|D| \geqslant 2$ is odd. Let the set of branchings $B = \{(d, d') | A^{(0,1)}(d, d') = 2\}$ be symmetric with respect to the diagonal of $A^{(0,1)}$ and contain it. Moreover, assume that the set B intersects each row at an odd number of entries. Let $A^{(0,1)}$ be antisymmetric off B, i.e.,

$$\{A^{(0,1)}(d, d'), A^{(0,1)}(d', d)\} = \{0, 1\} \qquad \text{for} \quad (d, d') \notin B$$

and let half of the elements on each row in the complement of B be 0's (and half 1's). Let $A^{(1,0)} = A^{(0,1)^T}$. The rest or the submatrices and Q are generated as in $\mathscr{AC}$. This class of CA is denoted by $\mathscr{ABC}$. The *branching intensity* of the boundary motion is $b = |B|/q^2$.

Remarks. Note that again the rule f, i.e., the full Cayley table, is symmetric. Conditioned on not branching, the motion of the boundary point is as in Theorem 2.4. From the fact that (d, d') is uniformly distributed in $D \times D$ and from the structure of $A^{(0,1)}$ it follows that the branching rate is simply the density of B in the off-diagonal submatrices. The matrix on the right in Table I is an example of a rule in $\mathscr{ABC}$ ($Q = \mathbf{Z}_3$ and the branching pairs B are on the diagonal in each $A^{(a,a')}$, $a \neq a'$).

In principle the class $\mathscr{ABC}$ can be used to generate arbitrarily potent random walk ensembles.

Proposition 2.6. Given any $b \in (0, 1]$ and $\varepsilon > 0$ there exists a CA in $\mathscr{ABC}$ such that its branching rate is within ε of b.

Proof. For a given b pick q a multiple of 3 and such that $1/q \leqslant b$ and $8/q^2 < \varepsilon$. Form a $3q \times 3q$ Cayley table in $\mathscr{ABC}$ such that in $A^{(0,1)}$ the diagonal branches and the rest is an asymmetric checkerboard of 0 and 1. For this rule $b = 1/q$. To build a rule with larger b, start filling in the branching entries (in each $A^{(a,a')}$, $a \neq a'$, i.e., staying in $\mathscr{ABC}$) first around the diagonal symmetrically, each time adding $6/q^2$. Once this is completed (in $q/3$ steps) continue flipping the remaining entries to 2 symmetrically in pairs of 2×2 squares, thereby increasing b by $8/q^2$ at a time. Once only overlapping squares can be placed, add them in a symmetric way so that they cover one 0 and 1 in each row and column. This can be continued up to $b = 1$. ∎

There are by no means all one-dimensional CA that generate good

defect gas dynamics, but rather prototype classes. It is perhaps appropriate to motivate some features by unveiling the "physical" ideas behind them.

The basic physical assumptions we implemented in the prototypes were:

(i) Isotropy, i.e., left–right symmetry of the interaction between the subalphabets.

(ii) The boundary motions should all be statistically identically identical and only their types should differ.

(iii) The individual boundary motions should be unbiased random walks with i.i.d. increments (and hence Markovian) and their characteristics, such as variance, branching rate, etc., should be computable.

As noted in the remarks, all the tables are symmetric, hence (i) is satisfied. Since all the interaction matrices between two subalphabets $A^{(a,a')}$, $a \neq a'$, are generated from a seed table $A^{(0,1)}$ as elements of the orbit under the permutation ϕ, they will be equivalent in branching and interaction properties. Of course we see this more directly from the proof of Theorem 2.4, which also shows that the choice of the distribution of 0's and 1's in $A^{(0,1)}$ in our classes guarantees a random walk of the type (iii). Note also that the permutation applied to the graph on the left in Fig. 2 yields an isomorphic graph.

Before elaborating on the dynamics of the CA we will note one additional feature of our design. By the invariance of the subalphabet $S^{(a)}$ the diagonal assignment matrix $A^{(a,a)}$ is constant. The violation of this, i.e., the existence of submatrices in the diagonal with $A^{(a,a)}$ $(d, d') \neq a$ for some (d, d'), amounts to the appearance of *spontaneous births* of twins, i.e., births of adjacent boundary points. The subsequent motions are of course still defined by the off-diagonal assignments together with the underlying digit dynamics. Since the diagonal blocks $A^{(a,a)}$ are not contributing to the characteristics of the boundary point motion, the distribution of the non-a entries is not relevant and the birth intensity is just the density of these entries in the submatrix. A prototype class, which we call $\mathscr{AB}$ (and could perhaps call *Ising*) exhibiting this phenomenon can be defined as follows: Suppose that $|A| = 2$, $|D|$ is even, and that off-diagonal assignments are as $\mathscr{AC}$. Let both matrices $A^{(a,a)}$ have density b of entries in the other subalphabet. Furthermore assume that at $b = 1/2$ the branching entries are distributed in such a fashion that the Cayley table becomes a quasigroup, i.e., every symbol appears on every row and column exactly once. This special condition will show its naturalness later. At this point we motivate it only by noting that the CA in class $\mathscr{ABC}$ are defined in a similar way—at $b = 1$ their Cayley tables are quasigroups.

3. DYNAMICS

We now present the analysis of the classes $\mathscr{AC}$, $\mathscr{ABC}$, $\mathscr{AB}$, and some of their more general relatives which all satisfy Assumption 1.3. Their dynamics as it appears in simulations is first briefly reviewed. After that we compare it with appropriate probabilistic models and note the conservation laws involved. The equilibrium properties pose some interesting problems which we report at the end.

3.1. Simulations

A series of computer simulations was first performed to confirm the qualitative behavior of the CA in the three prototype class as well as some rules outsides them and to measure the dependence of the dynamics on the parameters. The programs were written in *Mathematica* and run on a NeXTstation. In most simulations a toral universe maximum of 1000 cells in perimeter was initiated using a pseudorandom sample from an independent and uniform distribution on X. The length of the run was dependent on the birth/branching intensity—the lower the value of b, the longer the transient before equilibrium was attained. The range of runs was from 1000 to 9000 iterates. Although the backward cones of course start overlapping eventually, the long runs did not seem to reveal noticeable dependences due to this.

The critical finding was that *the underlying quasigroup structure is a sufficient condition for random walks to retain their qualitative and quantitative properties in the presence of others.* Our observations also strongly point toward it being a necessary condition. In its absence the random walk paths tend to corrupt to piecewise rectilinear motions, which indicates the existence of a measure concentrated on unidirectional cycles in the nodegraphs.[6] The asymmetry of the underlying quasigroup(s) as well as the constancy of $Q^{(a,a')}$ seemed irrelevant as anticipated. The assumptions on the assignment function $\underline{A}$ guarantee a simple (Markovian) structure for individual walks and this seems to be preserved for ensemble in the quasigroup case. The cardinalities $|D|$ and $|A|$ contribute as expected. The former influences the smoothness of the paths (the expected length of unidirected boundary pieces) and the latter just the number of boundary types available.

To illustrate the dynamics we have included some generic samples in Fig. 1. The top four represent 80×80 evolutions from fully disordered state (μ_S) on a toral universe. They are ordered from top left to middle right according to increasing branching rate, 0, 1/9, 1/3, and 7/9 respectively. The rules with $b = 0$ and 1/3 are the ones introduced in Example 2.1. The

former is in $\mathscr{AC}$ and the later is in $\mathscr{ABC}$. All the branching rules have $Q = \mathbf{Z}_3$. The rule with rate 7/9 is also in $\mathscr{ABC}$, while the one with $b = 1/9$ is just outside it ($|D| = 3$ implies $b \geqslant 1/3$ in $\mathscr{ABC}$—apart from having two nonbranching entries on the diagonals of $A^{(a,a')}$, the 1/9 rule satisfies the conditions in $\mathscr{ABC}$). The qualitative properties of the evolutions for automata with other values of b can be directly interpolated/extrapolated from these.

In the bottom row of Fig. 1 we have a second sample of evolution for $b = 1/3$ and 7/9 to further illustrate the domain formation in the branching case. The initial state is such that exactly two defects are present in otherwise disordered phases (i.e., probabilities on symbols within each subalphabet are uniform Bernoulli). By averaging over an ensemble of such branching trees for a given b value one concludes that the boundaries drift out at the correct rate $b/2$.

3.2. Probabilistic Analysis

The previous observations clearly suggest the existence of an attractor for the inert class $\mathscr{AC}$ and a nontrivial equilibrium measure for $\mathscr{ABC}$ and $\mathscr{AB}$. The structure of the attractor (candidate) is fairly easy to guess, as we will see, but to build a case for the latter we performed a series of runs cumulating data on the defect/particle density in a configuration and on the interparticle distance. These show a remarkably coherent picture under $\underline{A}$ and Q variation. We now present these findings along side an independent model.

Our model is defined on the same configuration spaces as our CA (X and $X^{(1/2)}$ alternating). Consider four adjacent lattice sites. As usual, if neighboring cells are in different subalphabets, there is a defect between them. Suppose that the defects are independently and uniformly distributed with density (frequency) ρ and that the center boundary is a defect. Assuming that all defects (at most three in our block) move to the left or right independently with equal probabilities and branch independently with probability b, we compute the number of descendants of the center defect in one iterate. By including all possible defect interactions within the four-block, we essentially compute a Feynman diagram and as a result get the density of deaths and births per lattice site as functions of the branching intensity and density of defects. In the steady state the densities of births and deaths have to match. The equilibrium solution of the defect versus the branching intensity is illustrated on the left in Fig. 3. See Appendix for details. The graph has several notable features, one of them being the fact that the value at $b = 1$, $\rho = 2/3$ is exact. This is a consequence of fact that this CA is permutive, thereby preserving the uniform Bernoulli measure.

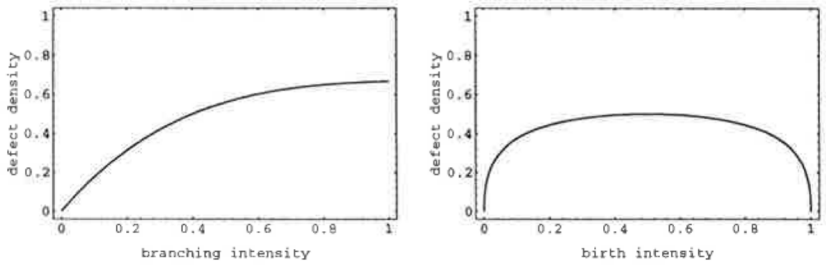

Fig. 3. Equilibrium densities in the independent models corresponding to $\mathscr{ABC}$ (left) and $\mathscr{AB}$ (right).

Hence the underlying independence assumption is satisfied. At $b = 0$ there is no mechanism to counter annihilations and coalescings and the asymptotic density should indeed be 0. Note the almost linear dependence on b at small values.

The graph corresponds with reasonably good accuracy to the data from CA runs. At large values of b the equilibrium particle density is very close to the value given by the model. At b values in (0.1, 0.6) the observed densities are within 5–15% of the ideal values. This seemed to hold for all sample CA independent of subalphabet size, quasigroup, and the particular distribution of the entries in the assignment function in $\mathscr{ABC}$. Even all examined assignment functions generating unbiased or minimally biased non-Markovian boundary motions (e.g., symmetric checkerboard off-B in $A^{(0.1)}$ in the branching case implies bias) given similar agreement with the model density $\rho(b)$. In the (0, 0.1) range the transient times made the density estimates less reliable, but there was nothing to indicate vanishing of $\rho(b)$ for some positive b, i.e., the existence of a nontrivial critical b value.

An obvious source of error is the fact that if two boundaries are at distance one from each other, then the probability that both branch may exceed b^2, the value in the independent case. This follows from the boundary pairs having a common digit. The mechanism does not plague boundary pairs further apart.

To see the basic phenomena in the case of births instead of branchings we only need to consider the interaction of two subalphabets. The ideal case involves the same independence assumptions as above together with the assumption that the cell boundaries in pure phase give rise to births independently with intensity b. Again the equilibrium density is exactly solvable (see Appendix). Its graph is shown on the right in Fig. 3. Since flipping of a fraction b of the cells in a given pure phase is equivalent to flipping the fraction $1 - b$ in the opposite phase, we see that the density must be symmetric with respect to $b = 1/2$. At small values, $\rho(b) \sim 2\sqrt{b}$.

The singularity of the derivative of ρ at 0 and 1 makes the comparison of the model to CA with birth mechanism somewhat unreliable at low and high birth rates. However, at the midrange of (0.2, 0.8) the observed match is comparable to that of the branching midrange. At the special value $b = 1/2$ the model is exact with $\rho = 1/2$.

The interparticle distance at the equilibrium gives more detailed information about the stationary measure. It also indicates the non-Markovianity (with respect to the spatial shift σ) of the measure when it is nontrivial, i.e., for parameter values $b \neq 0$ and 1 for $\mathscr{ABC}$ and also $b \neq 1/2$ for $\mathscr{AB}$. In Fig. 4 we plot the logarithm of the density of the distance distribution versus the interparticle distance at three different b levels. These are 1/3, 5/9, and 7/9, the first corresponding to the shallowest and the last to the steepest curve. Over one million defects were recorded for each curve and the tail of the distribution was cut at sample level one or at distance 40. The b values 1/3 and 7/9 correspond to the rules explained in Sections 2 and 3.1 and the third has the same quasigroup and with symmetric distribution of branchings in each $A^{(a,a')}$ as required for the class $\mathscr{ABC}$. Again we believe that the forms of the graphs are generic, i.e., essentially independent of Q, etc.

These data clearly indicate the non-Markovianity of the equilibrium measure. Suppose that the projection of the equilibrium measure on its first coordiniate, i.e., sequences in $A^{\mathbf{Z}}$, is ergodic and Markovian (with respect to the shift σ). If p_n denotes the probability of a contiguous block of length n of any symbol from A (i.e., the probability of having two defects n apart), then $p_n = \rho(1-\rho)^n$. Here ρ is as before

$$\Pr(\text{defect at site } j - 1/2) = \Pr(s_j \notin S^{(a)} \mid s_{j-1} \in S^{(a)})$$

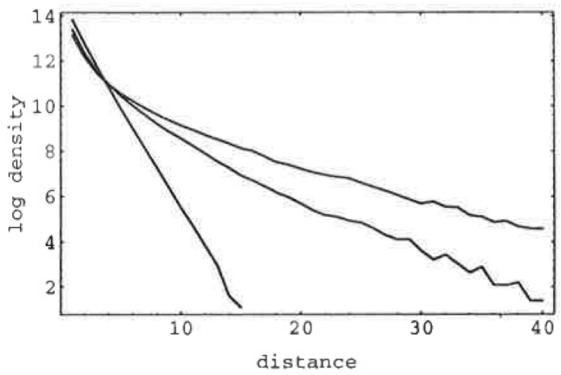

Fig. 4. Equilibrium interparticle distance distribution for $\mathscr{ABC}$. Branching rates corresponding to the curves, shallowest to steepest, $b = 1/3$, 5/9, and 7/9.

for any subalphabet a. But then the logarithm of the distance density should be linear, which does not seem to be the case (see Fig. 4).

The graphs suggest superimposition of at least two component distributions. For b near 1 an exponential distribution dominates. In fact at b value 1 the interparticle distance is exactly exponential (as a consequence of the rule being permutative, hence Bernoulli measure being preserved). At lower b values large contiguous blocks of pure phase will emerge and when they do they will persist for some time, thus contributing to the distribution the component so notably absent in the $b = 7/9$ graph.

The non-Markovianity of course points out a shortcoming in the computation of the densities in the beginning of the section. The independence assumption on the defect distribution is likely to have contributed to the deviation at low b values.

3.2. Conservation Laws

The main difficulty introduced in the transition from probabilistic particle systems to CA is that of conservation laws. They typically restrict the CA from having higher-order mixing properties, exponentially vanishing correlations, and similar useful properties. We now proceed to investigate these laws in our CA with the special goal of trying to understand why their total contribution to the dynamics does not seem to be proportional to their number.

The nature of the *digit-level* conservation laws can be best understood by considering the basic case of $Q = \mathbf{Z}_p$, p prime. Any single nonzero digit g at the origin surrounded by identity on $\mathbf{Z}_- \cup \mathbf{Z}_+$ generates a Pascal's triangle modulo p rooted at g on the top. This set will contain rows having just two g's in them at heights (measured from the top) p^k, $k \geqslant 0$. Moreover, these triangles for arbitrary root digit can be superimposed, i.e., added mod p. Hence for any j and any $i, k \geqslant 0$ it holds that

$$Q(d_{(j,i)}, d_{(j+p^k,i)}) = d_{(j+p^k/2, i+p^k)}$$

Indeed the existence of this dependence is the reason for the digit evolution not being three fold mixing.[12,11] Note that although there is an infinite number of these laws, their size (p^k) increases exponentially and requires the given exact geometric arrangement to prevail.

If we consider time and distance $l \neq p^k$ we arrive at a more complicated dependence relation involving also some of the digits between $d_{(j,i)}$ and $d_{(j+l,i)}$. This is a consequence of the fact that Pascal's triangle rooted at such digits can be nonzero at $(j + l/2,\ i + 1)$. But the density of any

Pascal's triangle (in the forward cone) vanishes as its height approaches infinity. Hence also these conservation laws are rare for large l.

The argument given here actually extends to other cyclic groups and, for example, to the Klein four-group. In the latter all nonidentity elements are of order two, so the argument for $\mathbf{Z}_2$ applies. Indeed loops, i.e., quasigroups with identity, are argued similarly.

Since our primary concern is the boundary motions we would like to know whether there are *increment-level* conservation laws. By this we mean relations between the increments (jump directions) at distinct boundary points. This does not seem to happen in general, but it is possible that a digit-level conservation law lifts. The case in point is $Q = \mathbf{Z}_2$ and an assignment as in class $\mathscr{AC}$. Consider an arrangement of boundary pairs centered at (j, i), $(j+2^k, i)$ and $(j+2^{k-1}, i+2^k)$. The reversal of the increment, say, at $(j+2^k, i)$ is caused by permutation of the digits in this boundary pair. But any such permutation also permutes the digits of the boundary pair at $(j+2^{k-1}, i+2^k)$ (the third pair is fixed). Hence there is a permutive relation between the increments in three different locations. However, this relation breaks down for bigger Q's, since the permutation does not lift from digits then. And it does not seem to make CA with quasigroup $\mathbf{Z}_2$ behave noticeably differently.

The conservation laws seem to cause significant consequences only if the CA is computed on a toral lattice of the wrong size. To see this, consider again the digit evolution in the case $Q = \mathbf{Z}_p$, p prime. Let d_i be the density of nonzero digits in the ith row of the Pascal's triangle. Drops in d_i happen at time (heights) $p, 2p, \ldots, p^2, p^2+p, \ldots, p^3, \ldots$. From the structure of the Pascal's triangle we see that large decreases in the density occur when for some $k \geqslant 1$, i/p^k is a small integer. Indeed if i is a power of p, d_i is close to zero, as there are exactly two nonzero entries on these lines (the case considered in the beginning).

A consequence of this is that if the perimeter of the torus T equals p^k for some k the digit evolution from any initial sequence is identically zero from time $i = p^k$ on, as the two digits alive in a Pascal's triangle rooted at any point of the initial configuration cancel each other. More generally, if p^k for some k is a big divisor of T, the density fluctuations in the digit evolution are further amplified from the nontoral case. These torus sizes should obviously be avoided.

3.3. Equilibrium

In view of the design principles of the CA classes as well as the results above we now venture to formulate the equilibrium behavior of the automata as well as the convergence to it.

A deterministic CA typically has multiple invariant measures. The simplest of the singular ones are supported by periodic points. Apart from a few exceptions, these seem in general have a vanishing basin of attraction and therefore are not of physical importance. If a rule has a nontrivial invariant subalphabet, the uniform Bernoulli measure on it is an invariant measure.[5] Very little seems to be known about any other types of invariant measures.

Once the trivial singular measures are excluded we expect the invariant measure characterization in our setup to be as in analogous classical statistical mechanical models. The omission is made by requiring that $\pi_2\mu$ is absolutely continuous (recall that given a measure μ on X, $\pi_2\mu$, is the coordinate projection on $D^{\mathbf{Z}}$). In the remaining set of measures we expect the rules in $\mathscr{AC}$ to be nonergodic and the rules in $\mathscr{AB}$ and $\mathscr{ABC}$ to be ergodic. Note that since the class $\mathscr{A}(\mathscr{C})$ can be viewed as the limit of the class $\mathscr{AB}$ as the birth rate approaches zero, the ergodic behavior is as in the none-dimensional Ising model.

To be more precise, we define two properties of good initial measures μ:

(i) $\mu = \mu_1\mu \times \mu_D$.

(ii) $\rho(x) > 0$ for μ-almost every x, where ρ stands for defect density.

Assumption (i) guarantees ideal digit dynamics, i.e., stationarity and maximal obtainable mixing, and the product form allows arbitrary defect distribution. The initial distribution of perhaps the main interest, the independent uniform measure on all symbols (μ_S), clearly satisfies both conditions. However, it may be of interest to also consider "quenched/enhanced" initial measures where the defect density has been altered within (ii).

Let $\mu^{(a)}$ be the uniform Bernoulli on $S^{(a)^{\mathbf{Z}}}$ and recall that the weak convergence of measures $\mu^i \Rightarrow \mu^*$ just requires $\int f\, d\mu^i \to \int f\, d\mu^*$ for bounded and continuous f. We let $F^i\mu$ stand for the measure defined as $(F^i\mu)(A) = \mu(F^{-i}A)$.

Conjecture. For every $F \in \mathscr{AC}$ and initial measure μ satisfy (i),

$$F^{2n}\mu \Rightarrow \mu^* = \sum_{a \in A} \lambda^{(a)}\mu^{(a)}$$

for $\lambda^{(a)} \geqslant 0$ and $\sum \lambda^{(a)} = 1$. If μ also satisfies (ii), then

$$\rho(F^n(x)) \sim \frac{c}{(\pi n)^{1/2}} \qquad \mu\text{-a.s.}$$

where $c = |A|/2 + \varepsilon$, $|\varepsilon|$ small.

For every $F \in \mathscr{ABC}$ there is an equilibrium measure μ^* ($F^2\mu^* = \mu^*$) such that $F^{2n}\mu \Rightarrow \mu^*$ for any μ satisfying (i) and (ii). For $0 < b < 1$ it is

a non-Markovian measure (with respect to the spatial shift σ) with equal density of subalphabets and with defect density in $(0, 2/3)$.

For $F \in \mathscr{AB}$ and $b \in (0, 1/2) \cup (1/2, 1)$ there exists an equilibrium measure μ^* such that $F^{2n}\mu \Rightarrow \mu^*$ for any μ satisfying (i). The subalphabets appear with equal density and the defect density is in $(0, 1/2)$.

Remark. The analogous statements obviously should hold for odd iterates, but we refrain from spelling them out, to avoid the extra indices.

Several points are in order to motivate and support the Conjecture. We also want to connect it to finding elsewhere.

The attractor in the class $\mathscr{AC}$ should simply be $A^* = \bigcup_{a \in A} S^{(a)\mathbf{Z}}$. The weights $\lambda^{(a)}$ and c in the Conjecture reflect the representation of the subalphabets in the initial measure, i.e., nonergodicity. In the even case (e.g., μ_S) one expects $\lambda^{(\cdot)} \equiv 1/|A|$ and $c \approx 3/2$. The latter assumes equal probabilities for annihilations and coalescings in recombinations. In case just two subalphabets are present, only annihilations take place and $c \approx 1$. Experimentally the bound for deviation ε is very small but hard to estimate reliably because of the slow convergence. Even in the case of biassed random walks the attractor should still be contained in A^* and the limit measure be of the given form. Due to the (standard) topology of the space (X, d) and the expected recurrence of the boundary motions the attraction is only in the mean, i.e., $(1/n)\sum_{i=0}^{n-1} d(F^{2i}x, A^*) \to 0$ μ-almost surely [use, e.g., the metric $d(x, x) = 0$, $d(x, y) = 2^{-\min\{|i| \mid x_i \neq y_i\}}$ on X].

For independent annihilating walks with independent exponentially distributed jumps a related result has been proved and should match our special case of two subalphabets.[10] If the sequences from $D^{\mathbf{Z}}$ under iteration of P were independent of each other a similar approach should work here. But by Theorem 2.2 the digit sets are just *asymptotically independent*. Indeed they are not 3-mixing, because of the conservation laws, but nevertheless the mixing rate is quite good and the resulting correlations (and length scale) are extremely small.

We also note that the first part of the Conjecture is closely related to Lind's conjectures on the elementary cellular automaton 18.[13] The rule 18 has permutivity properties completely explaining the individual random walks observed and the collective behavior seems to be that indicated in the Conjecture.[7,4] Indeed 18 has a quasigroup structure much the same as the rules in class $\mathscr{AC}$. To see this we present the Cayley table of 18 on the left in Table II.

The coding is $0 = 00$, $1 = 01$, etc., in terms of the original binary alphabet. The invariant subalphabets are $S^{(1)} = \{0, 1\}$ and $S^{(2)} = \{0, 2\}$. Clearly $f(s^{(1)}, s^{(2)}) \in \bigcup_a s^{(a)} \in S^{(a)}$. If the order of the subalphabets is reversed, we can get the symbol 3, but this is a redundant symbol. Its

Table II

0	1	2	2
1	0	0	0
2	3	0	0
1	0	0	0

0	1	2
1	0	0
2	0	0

0	1	$\hat{0}$	2
1	0	1	0
$\hat{0}$	1	$\hat{0}$	2
2	0	2	$\hat{0}$

appearance is avoided if the coding is started at odd location of $\mathbf{Z}$ instead of even ones. So the defects in 18 behave as in the CA with the table in the center. Furthermore, the ambiguity in the symbol 0 can be disposed of by defining a new symbol $\hat{0}$ for $S^{(2)}$ (this has no effect on the defect dynamics). The resulting table is on the right. The underlying quasigroup is clearly $\mathbf{Z}_2$. Although the assignment function is not as required in $\mathscr{AC}$, the subalphabets are evenly represented in $A^{(1,2)}$ and $A^{(2,1)}$ and an unbiased Markovian random walk prevails from the natural initial measure (as in Theorem 2.4).

The branching/birth mechanism in $\mathscr{ABC}/\mathscr{AB}$ makes the existence of a nontrivial equilibrium measure intuitively obvious. Note that because of the types of its offspring, a branching boundary cannot ever self-annihilate to extinction.

The nontrivial structure of μ^* conforms with earlier finding where the inert annihilating case with all independence assumptions was studied.[1] There it was shown that the defect distance at time n scaled by $\sqrt{n}$ does not converge to an exponential limit distribution. This corresponds to our finding on the increasingly non-Markovian nature of μ^* in the limit $b \to 0$.

Finally we remark that the cases $b = 1$ for $\mathscr{ABC}$ and $b = 1/2$ for $\mathscr{AB}$ are left out of the Conjecture since they are the only ones fully understood. The Cayley tables for these parameter values are quasigroups, the uniform Bernoulli measure on all of X is preserved, and the natural extensions of the CA are Bernoulli, i.e., maximally chaotic. Because of the measure preserved, the interparticle distance is exponential with mean 3/2 in $\mathscr{ABC}$ and 2 in $\mathscr{AB}$.

APPENDIX

The reference models of Section 3.2 assume that all the probabilistic mechanisms in the ensemble are independent of each other and of the past. So the increments of the defects are independent of the past of the ensemble and independent of each other up to the time of annihilation or coalescing. Similarly the branching or births are independent of the past, each other, and the increments.

Let ρ be the density of defects. With probability ρ we have a defect

at any given site. To obtain the density of defects after one iterate we consider a block of four cells centered at a defect. In the case of $\mathscr{ABC}$ the defect can jump by $\pm 1/2$ or branch. The offspring may annihilate or coalesce with neighboring defects if any are around. We compute the expected number of offspring by the center defect in one iterate after its interactions have been taken into account. For example, if in the case of three defects the center defect branches, the others move inward, and one of the children coalesces while the other annihilates, the number of offspring is 1/2 (as the child is parented by two defects). Given the density of defects, we can calculate the probability of this event to be $\rho^3 b(1-b)^2/8$. Note that the center defect could not interact with any nonneighboring defects in one iterate. Accounting for all possible events gives the updated defect density, which has to agree with ρ at the equilibrium. The argument can be further refined by taking into account the events where a branching is followed immediately (in one iterate) by a coalescing. With some computation this analysis leads to the equation

$$\left(\frac{b(-5-4b+9b^2)}{4}\right)\rho^2+\left(\frac{-3-2b+5b^2-12b^3}{2}\right)\rho$$

$$+b(3-2b+3b^2)=0$$

The nonnegative solution to this is the curve plotted on the left in Fig. 3. The contribution of the refinement is quite small—it just thins the distribution at the low end.

The case of births is dealt with similarly, but now without assuming that there necessarily is a defect in the center of a four-block of cells. We still count the number of offspring of the center (defect or not) and arrive at the equilibrium equation

$$[4b(1-b)-1]\,\rho^2-8b(1-b)\,\rho+4b(1-b)=0$$

Again there is only one physically meaningful solution, which is plotted in Fig. 3, right.

ACKNOWLEDGMENTS

The author woulds like to thank Mike Keane and Jeff Steif for conversations on related problems. This research was partially supported by the Academy of Finland and the Finnish Cultural Foundation.

REFERENCES

1. R. Arratia, Limiting point processes for rescalings of coalescing and annihilating random walks on $\mathbf{Z}^d$, *Ann. Prob.* **9**(6):900–936 (1981).
2. N. Boccara, J. Nasser, and M. Roger, *Phys. Rev. A* **44**(2):866 (1991).
3. M. Bramson and J. Lebowitz, Asymptotic behavior of densities for two-particle annihilating random walks, *J. Stat. Phys.* **62**:297–372 (1992), and references therein.
4. K. Eloranta, The interaction dynamics of the kinks in the cellular automaton Rule 18, Helsinki University of Technology, Institute of Mathematics, Research Report A 306 (1991).
5. K. Eloranta, Partially permutive cellular automata, *Nonlinearity* **6**(6):1009–1023 (1993).
6. K. Eloranta, Random walks in cellular automata, *Nonlinearity* **6**(6):1024–1036 (1993).
7. K. Eloranta and E. Nummelin, The kink of the elementary cellular automaton Rule 18 performs a random walk, *J. Stat. Phys.* **69**(5/6):1131–1136 (1992).
8. R. Fernández, J. Fröhlich, and A. Sokal, *Random Walks, Critical Phenomena, and Triviality in Quantum Field Theory* (Springer, Berlin, 1992).
9. P. Grassberger, New mechanism for deterministic diffusion, *Phys. Rev. A* **28**:3666–3667 (1983); Chaos and diffusion in deterministic cellular automata, *Physica D* **10**:52–58 (1984).
10. D. Griffeath, *Additive and Cancellative Interacting Particle Systems* (Springer, Berlin, 1979).
11. B. Kitchens and K. Schmidt, Markov subgroups of $(\mathbf{Z}/2\mathbf{Z})^{\mathbf{Z}^2}$, *Contemp. Math.* **135**:265–283 (1992).
12. F. Ledrappier, Un champ Markovien peut être d'entropie nulle et mélangeant, *C. R. Acad. Sc. Paris A* **287**:561–562 (1978).
13. D. A. Lind, Applications of ergodic theory and sofic systems to cellular automata, *Physica D* **10**:36–44 (1984).
14. K. Petersen, *Ergodic Theory* (Cambridge University Press, Cambridge, 1983).
15. V. Privman, Model of cluster growth and phase separation: Exact results in one dimension, *J. Stat. Phys.* **69**(3/4) (1992).
16. M. A. Shereshevsky, Ergodic properties of certain surjective cellular automata, preprint University of Warwick (1991).

Printed by Catherine Press, Ltd., Tempelhof 41, B-8000 Brugge, Belgium